PERGAMON

Journal of Structural Geology 25 (2003) 333–344

JOURNAL OF STRUCTURAL GEOLOGY

www.elsevier.com/locate/jsg

A conceptual model for the origin of fault damage zone structures in high-porosity sandstone

Zoe K. Shipton*, Patience A. Cowie

Department of Geology & Geophysics, Edinburgh University, West Mains Road, Edinburgh EH9 3JW, UK

Received 24 July 2001; received in revised form 1 March 2002; accepted 5 March 2002

Abstract

We present a conceptual model to explain the development of damage zones around faults in high-porosity sandstones. Damage zone deformation has been particularly well constrained for two 4-km-long normal faults formed in the Navajo Sandstone of central Utah, USA. For these faults the width of the damage zone increases with fault throw (for throws ranging from 0 to 30 m) but the maximum deformation density within the damage zone is independent of throw. To explain these data we modify a previously published theoretical model for fault growth in which displacement accumulates by repeated slip events on patches of the fault plane. The modifications are based on field observations of deformation mechanisms within the Navajo Sandstone, the throw profiles of the faults, and inferences concerning likely slip-patch dimensions. Zones of enhanced stress are generated around the tips of each slipping patch, raising the shear stress on adjacent portions of the fault as well as potentially causing off-fault damage. A key ingredient in our model for off-fault damage accumulation is the transition from strain hardening associated with deformation band development, to localised strain softening as a slip-surface develops. This transition occurs at a critical value of deformation density. Once a new slip-surface develops at some distance from the main fault plane and it starts to accumulate throw it can, in turn, generate its own damage zone, thus increasing the overall damage zone width. Our approach can be applied to interpret damage zone development around any fault as long as the host-rock lithology, porosity and deformation mechanisms are taken into consideration.

Keywords: Fault growth; Damage zone; Deformation bands

1. Introduction

Faults are often surrounded by a zone of subsidiary structures referred to as the damage zone (Chester and Logan, 1986). Possible origins for damage zone structures include flexure of beds around faults (Jamison and Stearns, 1982; Antonellini and Aydin, 1994), repeated slip on a fault surface (Vermilye and Scholz, 1998), enhanced stress at fault tips (Cox and Scholz, 1988; McGrath and Davison, 1995; Martel and Boger, 1998; Vermilye and Scholz, 1998) and strain at zones where adjacent fault segments link (Peacock and Sanderson, 1991; Childs et al., 1995). Recognition of systematics in the geometry of damage zone structures would aid in the prediction of sub-seismic fault distribution (e.g. Knipe et al., 1998) and the characterisation of fluid flow within and around fault zones (e.g. Caine et al., 1996; Shipton et al., 2002).

A detailed investigation of damage zone structure around kilometre-scale faults in the high-porosity (20%) Navajo Sandstone found that damage zone width was proportional to the total fault throw (Shipton and Cowie, 2001). Similar positive correlations have also been found in other high-porosity sandstones (Knott et al., 1996; Beach et al., 1997, 1999; Myers and Aydin, 1998; Fossen and Hesthammer, 2000) and in mixed sedimentary sequences (Wallace and Morris, 1986). Knott et al. (1996) discussed the effect of extensional and compactional quadrants around growing faults on the width of the resulting damage zone. However, the role of deformation mechanisms in controlling the scaling of damage zone width and displacement has not previously been discussed.

A model proposed by Cowie and Shipton (1998) conceives of fault growth as occurring by repeated slip on many small patches of the fault surface. This model successfully demonstrated that observed fault displacement profiles (e.g. Muraoka and Kamata, 1983; Dawers et al., 1993; Cartwright and Mansfield, 1998) can be modelled by the summation of many small slip events without creating unrealistic stress concentrations at the fault tip (Cowie and Scholz, 1992). As we show here, this model also has

* Corresponding author. Now at: Department of Geology, Trinity College, Dublin 2, Ireland.

E-mail addresses: shiptonz@tcd.ie (Z.K. Shipton).

0191-8141/03/$ - see front matter © 2002 Elsevier Science Ltd. All rights reserved.
PII: S0191-8141(02)00037-8

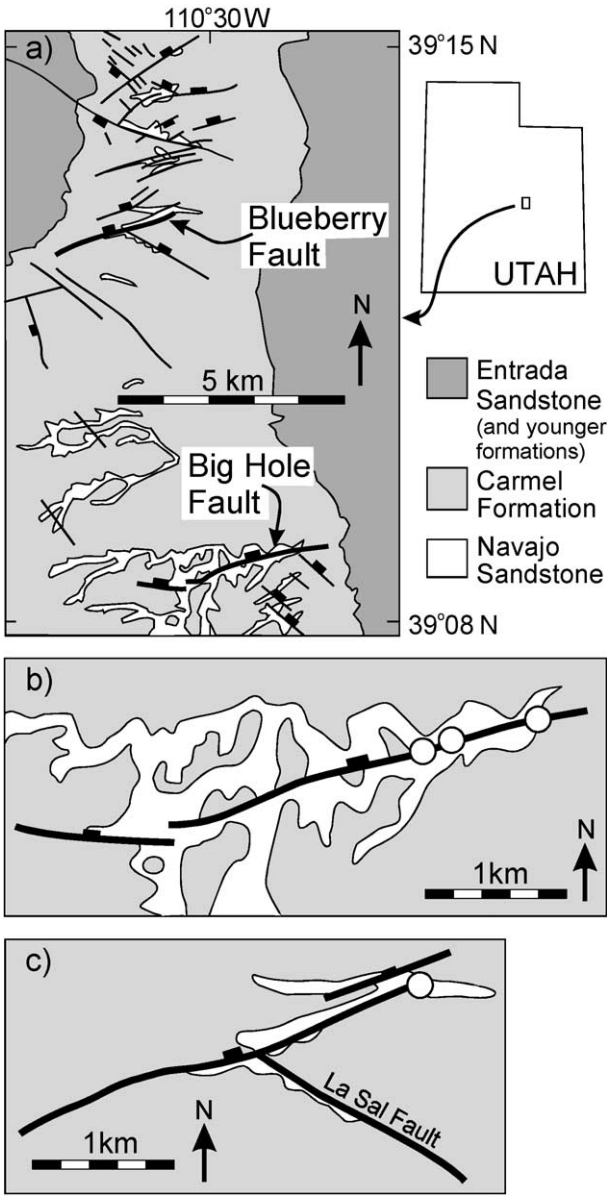

Fig. 1. Location map of the study area (a) and close up maps of (b) the Big Hole fault and (c) the Blueberry fault with the detailed study sites shown as white circles.

important implications for the development of damage zone structures. When a slip-patch ruptures, stress is enhanced in a volume around the slip-patch tip. In addition to re-loading the fault plane along strike, this could cause failure of the rock out of the plane of the fault. In this paper we investigate the implications of this slip-patch model for the distribution, geometry and evolution of damage zone structures.

We start by presenting field data collected from two 4-km-long faults that provide a particularly well-constrained example of fault damage zone structures in high-porosity sandstone (Shipton and Cowie, 2001). We then summarise the slip-patch model presented in Cowie and Shipton (1998) and discuss the implications of the modified slip-patch fault growth model that includes strain hardening to explain the generation of the damage zone in our study area. Finally we discuss the potential for applying this model to other faults.

2. Field observations

2.1. Field setting

The Big Hole and Blueberry faults in the Chimney Rock fault array, central Utah, have exceptional along-strike exposures of damage zone structures (Fig. 1). Both faults are several kilometres in length with maximum throws of tens of metres. Cowie and Shipton (1998) presented high-resolution measurements of throw on the Blueberry fault and Shipton and Cowie (2001) presented throw profiles and maps of the damage zone from both the Big Hole and Blueberry faults. The faults cut the Jurassic Navajo Sandstone, a medium-grained aeolian arenite with an average porosity of 20% (Dunn et al., 1973; Shipton and Cowie, 2001). The excellent outcrops of the damage zones of these faults allow us to investigate the development of damage zone structures with increasing displacement.

Both faults have simple symmetrical throw profiles characteristic of isolated faults (Dawers and Anders, 1995; Nicol et al., 1996). The eastern end of the Big Hole fault does not appear to link with any other faults along strike although the tip region is buried beneath Quaternary sediments. In contrast the tip of the Blueberry fault is well exposed. Because the Big Hole and Blueberry faults are of similar size and have similar throw gradients, we treat the Blueberry fault tip as a proxy for the tip of the Big Hole fault giving a range of fault throws from 0 to 30 m (Fig. 2).

2.2. The damage zone

The Big Hole and Blueberry fault zones consist of a fault core surrounded by a damage zone comprised of clusters of deformation bands (Fig. 2). Deformation bands are ~1-mm-thick zones of cataclasis and are the typical deformation element in high-porosity sandstones (Aydin, 1978; Aydin and Johnson 1978, 1983; Antonellini and Aydin, 1994). The fault core consists of tightly packed deformation bands, often bounded by thin (<1 mm thick), highly polished, slip-surfaces. Slip-surfaces have distinctly different microstructures compared with the deformation bands (Aydin and Johnson, 1983; Shipton and Cowie, 2001), and they accommodate substantially more offset (up to 30 m along these faults). One or more primary slip-surfaces can be identified within the fault core, and these are the surfaces upon which the majority of the fault offset is accommodated. In the rest of the paper we refer to this feature as the main fault plane. In the damage zone, discontinuous slip-surfaces occur within deformation band clusters, and have offsets that are typically between 30 and 200 cm (Shipton and Cowie, 2001).

The damage zone is therefore comprised of deformation band clusters and occasional slip-surfaces, along with a

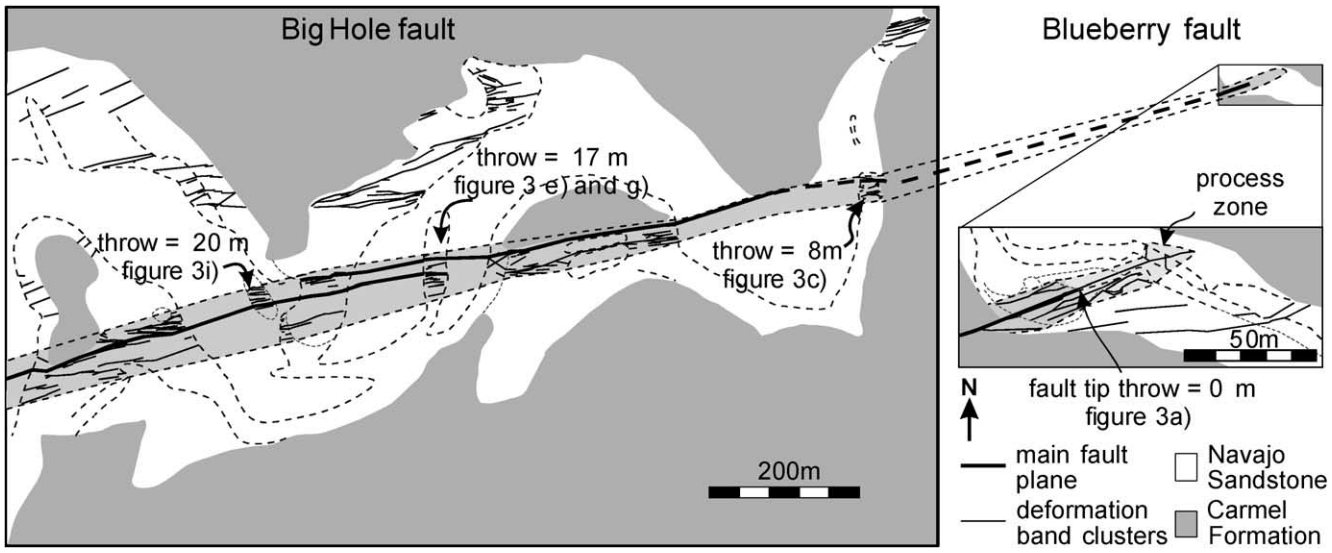

Fig. 2. Damage zone maps for the Big Hole and the Blueberry faults (from Shipton and Cowie, 2001). Clusters of deformation bands (thin black lines) define the damage zone (pale grey area) around the main fault plane (thick black lines). Outside this zone deformation band clusters are rare. Dotted grey lines show the extent of outcrop. Small map on the right shows the Blueberry fault map at the scale of the Big Hole map (left hand side) plotted at the projected position of the eastern tip of the Big Hole fault. The detailed study site locations are shown with the throw on the fault at that point.

proportion of relatively undeformed host rock. Outside this damage zone the rock is essentially undeformed: there are no longer any deformation band clusters and only very sparse, isolated, single deformation bands. This transition from deformation band clusters to few or no deformation bands defines the edge of the damage zone (Fig. 2). The proportion of strain that is taken up by the damage zone compared with the main slip-surface of the fault is not precisely known. However, given that deformation bands are never seen to have large slips and that slip-surfaces within the damage zone are relatively few in number and not laterally extensive (Fig. 2), it is clear that the majority of the throw measured on the top Navajo Sandstone is taken up on the main fault plane.

The geometry of structures within the damage zone of the Big Hole and Blueberry faults indicates that damage zone development is due to the process of displacement accumulation on the main fault surface. Firstly, deformation band clusters dip synthetically and antithetically to the main fault, but are not strike parallel. This variation in strike is symmetrical around the main fault plane defining an orthorhombic symmetry, which implies that they formed within a three-dimensional strain field (Reches, 1983; Krantz, 1988; Shipton and Cowie, 2001). For orthorhombic dip-slip normal faults, the angle between strike sets, α, is proportional to the ratio of the horizontal strains, k. The low angle between the strikes of deformation band clusters in the Big Hole and Blueberry fault damage zones ($\alpha = 8$ and $11.5°$, respectively) can be explained in terms of a component of fault-parallel extension that is much smaller than the fault-perpendicular extensional strain. For the Big Hole fault $k = -0.02$ whereas $k = -0.04$ for the Blueberry fault tip (see Shipton and Cowie (2001) for more details). The orientations of damage zone structures are significantly different from those due to the regional strain field ($k = -0.16$, $\alpha = 24°$; Krantz, 1988). Thus, we interpret the damage zone structures to have formed in a locally controlled strain field due to growth of these faults.

Secondly, Shipton and Cowie (2001) showed that damage zone width varies along the faults such that on average the width, w, is approximately two and half times the throw, t, i.e. $w = 2.6t + 7.2$ (both w and t measured in metres). Damage zone width data from five drill holes through the covered eastern end of the Big Hole fault (Shipton et al., 2002) also fit this correlation. Note that there is significant scatter associated with this scaling relationship, allowing a variation in width of 10–20% for any given value of throw. However, the overall positive correlation suggests that the damage zone results from a process of displacement accumulation on the main fault plane, and thus fault growth. The damage zone is approximately 12 m wide at the Blueberry fault tip where measurable displacement has not yet accumulated (Fig. 2). Because deformation ahead of the fault tip cannot be a direct result of displacement accumulation, we interpret it as deformation associated with tip propagation, i.e. the process zone.

2.3. Deformation density

The variation of deformation density within the damage zone is a convenient way of describing local variations in strain. Deformation density is defined as the number of features per unit area. This measure is distinct from deformation intensity, which is the density multiplied by the offset on each feature (Jamison and Stearns, 1982). Intensity is more difficult to constrain because the offset is harder to

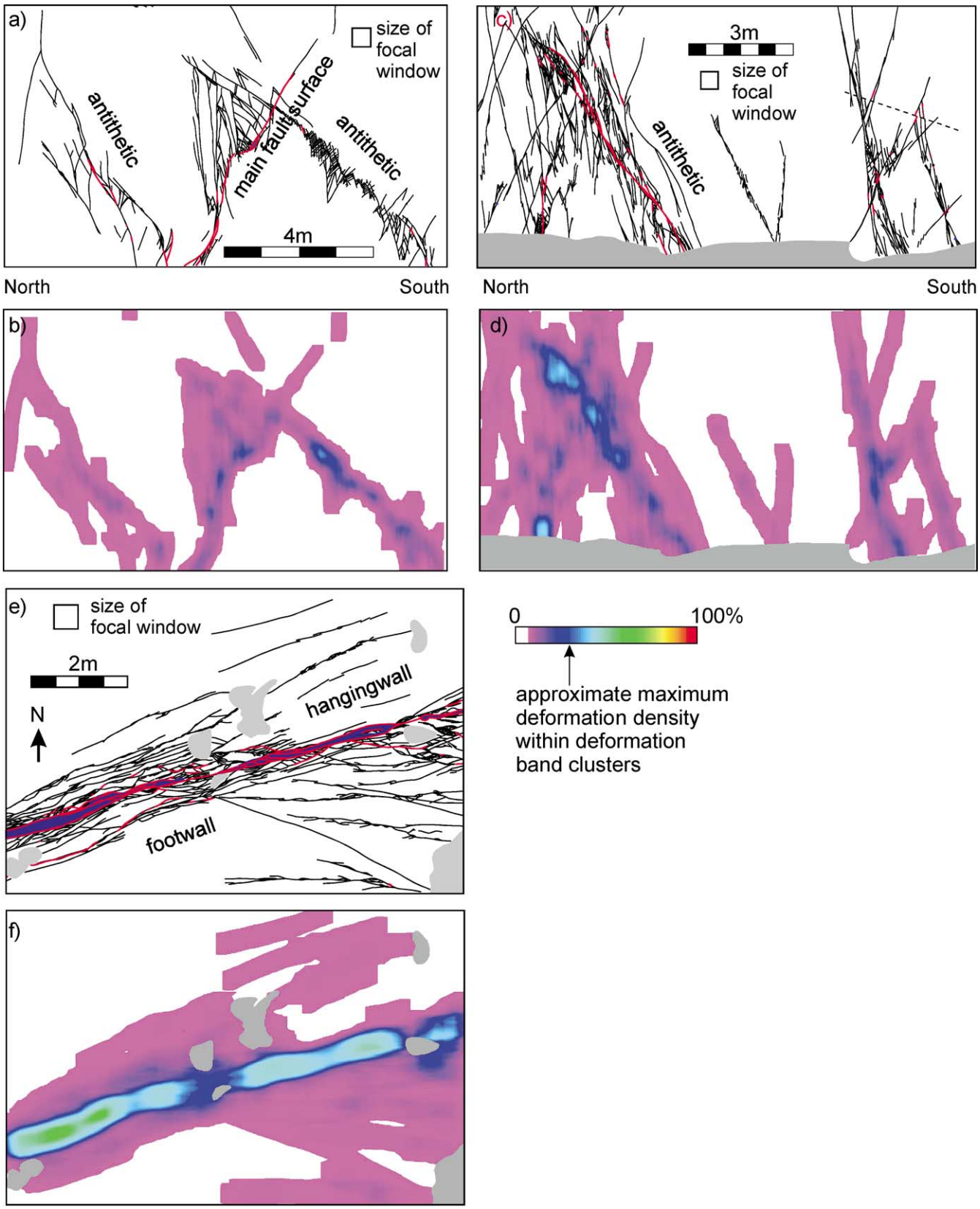

Fig. 3. Outcrop maps and deformation density maps for (a) and (b) the Blueberry fault tip (throw = 0 m), (c) and (d) the 8-m-throw site on the Big Hole fault (main fault plane is 1 m to the left of this image), (e) and (f) the 17-m-throw site on the Big Hole fault (northern strand with throw ≈ 3 m), (g) and (h) the 17-m-throw site on the Big Hole fault (southern strand with throw ≈ 14 m), (i) and (j) the 20-m-throw site on the Big Hole fault. Note that the southern strand of the Big Hole fault at the 17-m-throw site is defined as the main fault plane as it accounts for 82% of the total throw at this point. Deformation bands, slip-surfaces and fault core are colour-coded black, red and blue, respectively, in outcrop maps (a), (c), (e), (g) and (i). Colour scale in deformation density maps ranges from white = 0% deformation to red = 100% deformation. Some local maxima are edge effects where the focal window contains a large proportion of 'no data' points and the focal mean returns artificially higher values of density. Outcrop maps from Shipton and Cowie (2001).

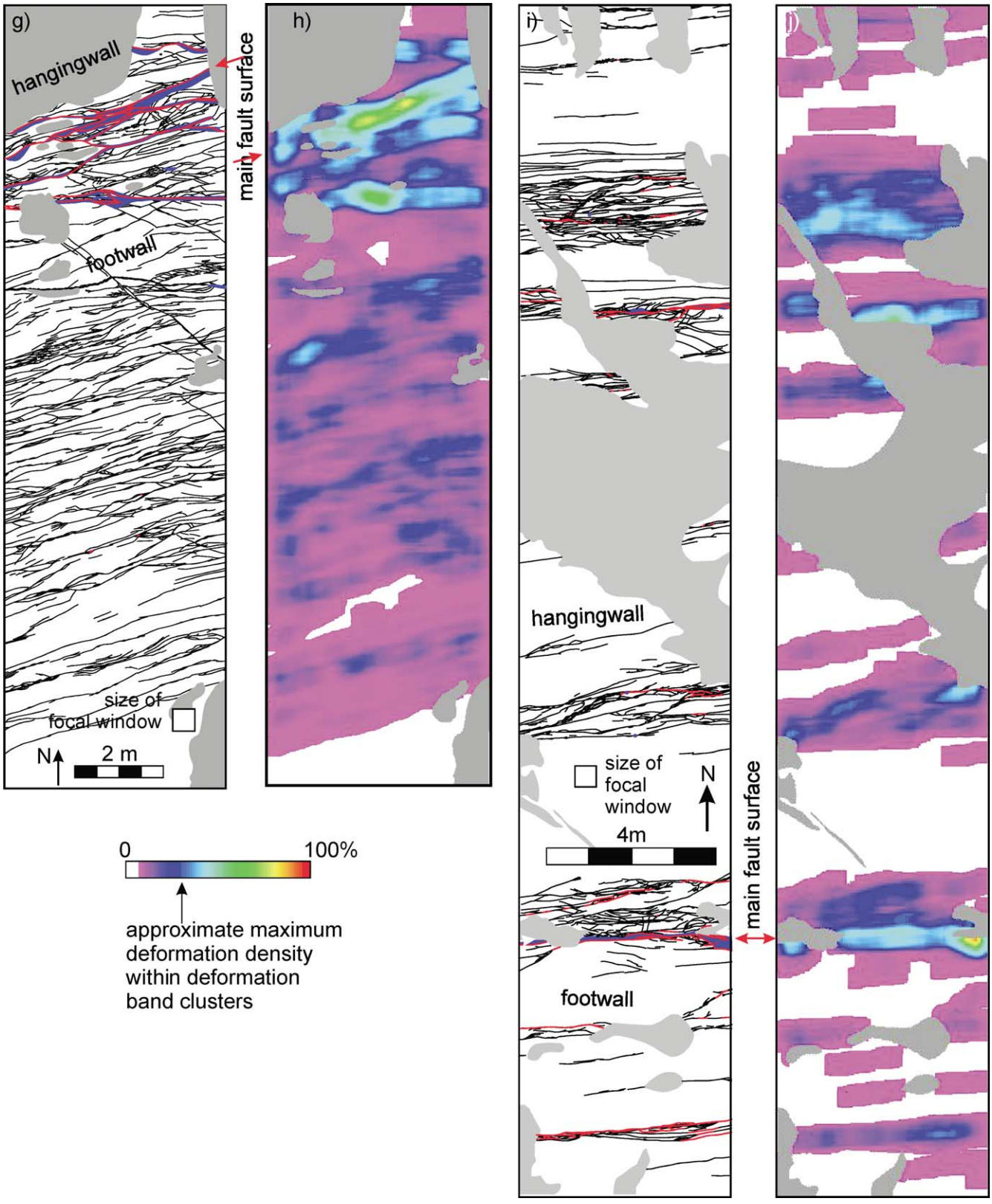

Fig. 3. (*continued*)

measure and can be prone to significant uncertainty. Digitised line drawings of individual outcrops (Shipton, 1999; Shipton and Cowie, 2001) were analysed using the image analysis package Erdas Imagine. The results of this analysis are contour plots of deformation density (Fig. 3). Deformation density is calculated by first assigning a value to each pixel of the image, which for these images represent 7 mm in real space. Deformation bands, slip-surfaces and fault core (colour-coded black, red and blue, respectively, in Fig 3a, c, e, g and i) and are assigned the value 100. Areas of outcrop with no visible deformation (white areas in Fig. 3) are assigned the value 0. Areas where the outcrop is covered are shown as grey in Fig. 3 and are assigned the value 101, i.e., no data. The area over which density is calculated is called the focal window and for the contour plots shown in Fig. 3 is 0.25 m^2. For each pixel in the image we calculate the focal mean, which is the mean value of all the pixels within the focal window excluding pixels with 'no data' values = 101 (grey pixels). The focal mean is thus equivalent to the deformation density for this size of focal window, i.e., the percentage area of uncovered outcrop within the focal window that contains deformation.

The deformation density values that we obtain do depend on the size of the focal window used, but the actual values are not of as much interest as their distribution. We can only use the results of this type of analysis to assess relative variations in deformation density at a given scale, in this case 0.5 m. Fig. 3 shows the results of our analysis for five locations in the damage zone over a range of values of throw on the fault, from the tip (Fig. 3a, b; throw = 0 m) to near the fault centre (Fig. 3i and j; throw = 20 m).

The damage density maps show several key features. Firstly, deformation within the damage zone is clustered, with areas of no deformation between zones of deformation band clusters. Secondly, at this scale the *maximum* deformation density within the damage zone clusters is fairly constant, (Fig. 3b, d, f, h and j). Blue colours (~30% deformation band density) are generally associated with clusters of deformation bands with either no slip-surfaces, or with short isolated slip surfaces. The turquoise areas (~40% deformation band density) represent the highest density of deformation bands clusters where slip-surface development is, in general, more pronounced with incipient linkage of neighbouring slip surfaces. Some local maxima are edge effects where the focal window overlaps a large area of no outcrop and the focal mean returns artificially high values of density. These are < 1 m in size and occur where there are no slip-surfaces apparent. Thirdly, there appears to be a positive correlation between the number (and continuity) of slip-surfaces within the damage zone and the throw on the main fault surface (Fig. 3; Shipton and Cowie, 2001). In contrast to the damage zone, in areas where many through-going slip-surfaces are concentrated along and immediately adjacent to the fault core, the deformation density is much higher (60–80%) indicated by green–yellow colours in Fig. 3b, d, f, h and j. The *maximum* width of the fault core (~30 cm) does not correlate with fault throw along-strike, and the width may be much less than this locally (Fig. 3).

Fig. 4 summarises these observations in an idealised 3-D diagram. We observe that (1) within the damage zone there is an approximately constant maximum deformation density, and (2) where throw on the fault is greater, the damage zone is wider and the number of slip surfaces increases, but there is no increase in the maximum deformation density. In the following sections we show how these observations may be interpreted in the context of throw accumulation on the Big Hole and Blueberry faults.

3. The slip-patch model of fault growth

Most seismically active faults rarely slip along their entire length; instead, portions of the fault surface rupture in one earthquake (e.g. Crone and Haller, 1991). It is therefore not appropriate for fault models to be constrained by assuming that failure always occurs over the entire fault surface (e.g. Pollard and Segall, 1987; Cowie and Scholz, 1992; Scholz et al., 1993; Bürgmann et al., 1994). Although earthquake ruptures can often terminate at segment boundaries (see Machette et al., 1991), many ruptures do not terminate at recognisable structural irregularities (dePolo et al., 1991; Roberts, 1996b). Therefore fault geometry is not the only control on rupture size. Small or aseismic faults can also grow by repeated rupture of small portions of the fault surface. Cross-cutting microfracture sets around small faults (0.8–40 m long) led Vermilye and Scholz (1998) to conclude that these faults had grown by repeated propagation of ruptures that were smaller than the length of the fault. Thus growth by multiple slip events along patches of the fault plane (e.g. earthquake ruptures) is a common growth mechanism in real faults.

Cowie and Shipton (1998) developed a 2-D numerical model to reproduce observed fault throw profiles, in particular to model fault tip throw gradients. This model idealises a fault plane as consisting of a linear array of elements with randomly varying strengths. As the fault is loaded, the weakest element will fail first. This failure results in a reduction of stress locally, and stress is transferred to neighbouring elements. Rupture on a small patch of a fault will relieve the stress on that portion of the fault but results in loading of adjacent areas (Fig. 5) (e.g. Stein and Lisowski, 1983; Martel and Pollard, 1989; Gupta and Scholz, 2000). The broken element is healed instantaneously by assigning it a new strength drawn from the initial strength distribution. As a consequence of the healing of slip-patches, previously ruptured areas can support subsequent loading. When these slip events are summed over time, the symmetry of the reloading results in an approximately symmetrical throw profile with linear tip throw gradients. In this model the fault propagates bilaterally so that the 'oldest' part of the fault is near the centre where the throw is greatest and the 'youngest' parts of the fault are near the tips where the

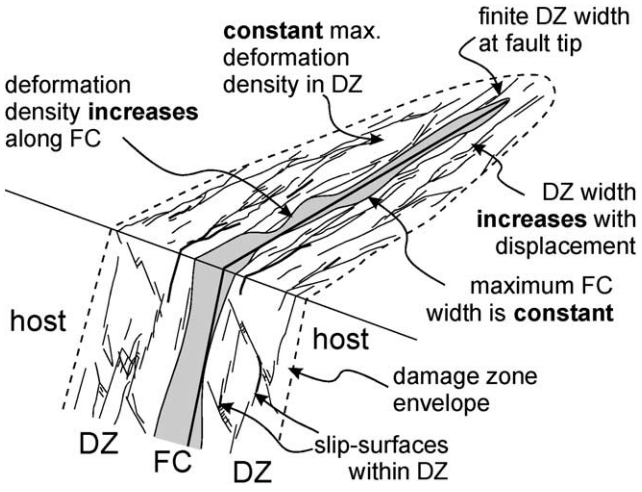

Fig. 4. Cartoon summarising the field observations. These relate to the scaling of damage zone width and deformation density with throw observed in plan view. The details of cross-sectional scaling are not resolvable in these outcrops, and the cross-section is shown merely to emphasise the orthorhombic nature of deformation band clusters within the damage zone. Slip-surfaces are shown as darker lines in the deformation band clusters. DZ = damage zone; FC = fault core.

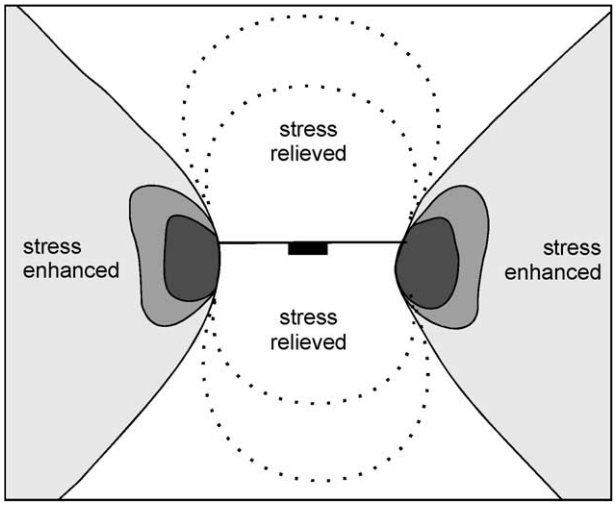

Fig. 5. Plan view of the stress change around a steeply dipping normal fault (after Hodgkinson et al., 1996). Regions of positive stress change (i.e. stress enhancement) are indicated by grey shading, areas of negative stress change (i.e. stress shadow) are indicated by dotted lines. If the stress around the tip exceeds the yield strength of the rock then deformation may occur within the region of stress enhancement.

throws are small. Note that the location of the maximum throw on the fault can vary with time.

3.1. Implications of the slip-patch model for damage zone structures

The slip-patch model described above assumes a planar 2-D fault and ignores out-of-plane deformation. Here we extend the model to consider the damage zone deformation that would be inferred from such a model. Deformation may be produced off the fault plane if the stress concentration in the volume around the tip of a slip-patch exceeds the local yield strength of the rock (Fig. 5). This off-fault loading effect can be seen in the distribution of aftershocks around an earthquake rupture (Scholz, 1990, p. 206; King et al., 1994; Hodgkinson et al., 1996). The size of the region of enhanced stress, and hence the width of the damage zone, should scale with the size of the slip-patches (Martel and Pollard, 1989). Thus the shape of the resulting damage zone produced by the original slip-patch model only depends on the relative size of the slip-patches as the fault grows.

If the slip-patches are all the same size and are small compared with the fault length (as in Cowie and Shipton, 1998), then a damage zone of constant, relatively narrow width would be expected to occur adjacent to the main fault surface (Fig. 6a). Furthermore, as there have been more rupture events at the centre of the fault than at the tip we would predict that the density of deformation in the damage zone should scale positively with the throw on the fault. Alternatively the fault could fail by slip-patches of all possible sizes, up to and including the size of the fault, located at any position along the fault (Fig. 6b). Because stress enhancement takes place preferentially at the ends of the slip-patch, the largest slip-patches would not cause damage at the centre of the fault. Superimposing these slip-patches therefore results in a damage zone that is wider at the fault tips (Fig. 6b). However, because more slip events take place at the centre of the fault there would be a greater density of deformation in this area even though the width of the damage zone is less than at the tips. None of the above scenarios can explain the observations described in Section 2 (Fig. 6c). Although the observed correlation between damage zone width and fault throw might be explained by arguing that large ruptures occur only along the central portion of the fault and small ruptures near the tip, there is no field evidence to support such an assumption, e.g. no variation in fault roughness along-strike (Shipton and Cowie, 2001). Consequently, an alternative explanation must be sought to explain the field observations.

4. A modified slip-patch model for the Big Hole and Blueberry faults

The structures in and around the Big Hole and Blueberry faults are consistent with the two main assumptions of the slip-patch model, i.e. that the fault slips repeatedly in small patches and that healing occurs, which allows stress to be supported on the fault surface. Microstructures in the fault zone illustrate that it has had a complex history of overprinting slip events. Very low porosity (a high degree of grain crushing) is seen in the cataclasite adjacent to the main fault slip-surface (fault core). This is overprinted with open microfractures and Riedel shears in orientations that suggest that they formed due to dip-slip shear parallel to the fault (Shipton, 1999). Multiple cross-cutting

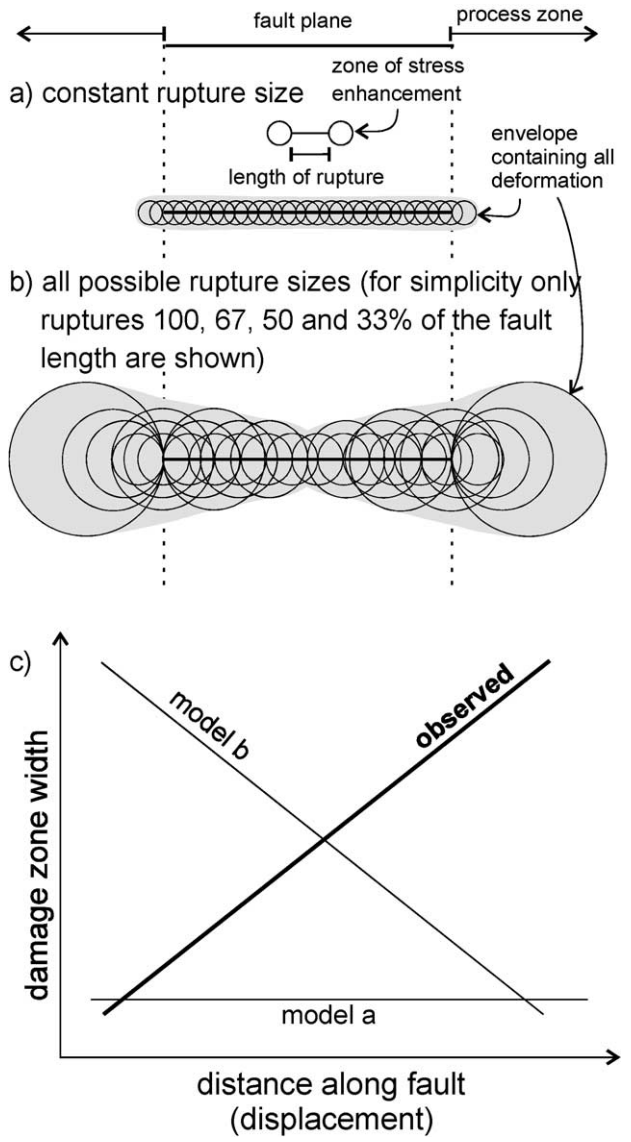

Fig. 6. Schematic representation of the distribution of damage zone deformation produced due to enhanced stress at the termination of slip-patches shorter than the length of the fault. Two possible scenarios are shown: (a) many small slip-patches of a constant size, (b) slip patches of all possible sizes up to and including the size of the fault. For simplicity the area of enhanced stress is shown as circular. The grey area is the damage zone resulting from the summed effect of all the ruptures. The process zone is the deformation ahead of the fault tip. (c) Scaling of damage zone width versus distance along the fault (i.e. throw) for the models shown above. Neither of these scenarios produces the positive scaling of damage zone width with throw seen for the Big Hole and Blueberry faults (bold line).

relationships between the deformation bands around the main fault surface also confirm that the fault has grown by multiple slip events (Shipton and Cowie, 2001). Concerning the issue of fault healing, borehole data from the Big Hole fault show that slip-surfaces are usually cemented at depth indicating that some form of chemical healing has occurred (Shipton et al., 2002). In addition, physical healing (interlocking of asperities, grain crushing etc.) will have been important in this lithology as evidenced by the strain-hardening deformation bands (Mair et al., 2000; Main et al., 2001) and cataclastic fault core.

According to the model of Cowie and Shipton (1998), the size of a typical slip patch may be inferred from the size of the fault process zone. This is because only slip-patches that rupture close to the tip of the fault will produce significant stress enhancement ahead of the tip (Fig. 6). The process zone width is therefore an indication of the dimensions of the last slip-patch to have ruptured close to the tip. The process zone deformation at the Blueberry fault tip consists of macroscopic deformation bands in a zone 12 m wide and 45 m long (Fig. 2). If, as argued by Cowie and Scholz (1992), the zone of enhanced stress around a rupture tip is approximately 10% of the length of the slip-patch then we infer the typical slip-patch dimensions to be in the range 120–450 m long.

4.1. The importance of strain hardening versus strain localisation

The observation of a constant maximum deformation density within the fault damage zone, combined with the correlation of damage zone width with throw, suggests that some process is transferring deformation away from the main fault with each repeated slip event. We suggest that this process may involve the competing effects of strain hardening and strain softening within this lithology. Strain hardening due to cataclasis and interlocking of crushed grains has been invoked to explain the formation of deformation bands (Aydin, 1978; Mair et al., 2000). This mechanism is active in the formation of deformation bands and zones of bands until a slip-surface nucleates, at which point the mechanism becomes locally strain softening and significant offset can accumulate (Mair et al., 2000; Main et al., 2001; Shipton and Cowie, 2001).

The transition from strain hardening to strain softening and localisation is vital to the overall development of the fault damage zone in this lithology. Repeated slip on the main fault plane causes additional deformation bands to form in the damage zone. Due to strain hardening, damage is preferentially located in undeformed host rock so the deformation density increases. Small isolated slip surfaces within the damage zone may also nucleate at this stage. However, when the deformation density at any point within the damage zone reaches a critical value (30% in our analysis, see Fig. 3), an interconnected slip surface develops away from the main fault and begins to localise some of the total throw across the zone (patch B in Fig. 7). This new slip surface can, in turn, generate more damage when it ruptures, further increasing the deformation density in adjacent areas. The width of the damage zone will increase as fault throw increases because the critical value of deformation density will be reached at progressively greater and greater distances from the main fault as throw accumulates and slip-surfaces within the damage zone gradually develop. This model implies a hierarchy of slip-surface development with distance from the main fault, i.e. better-developed slip

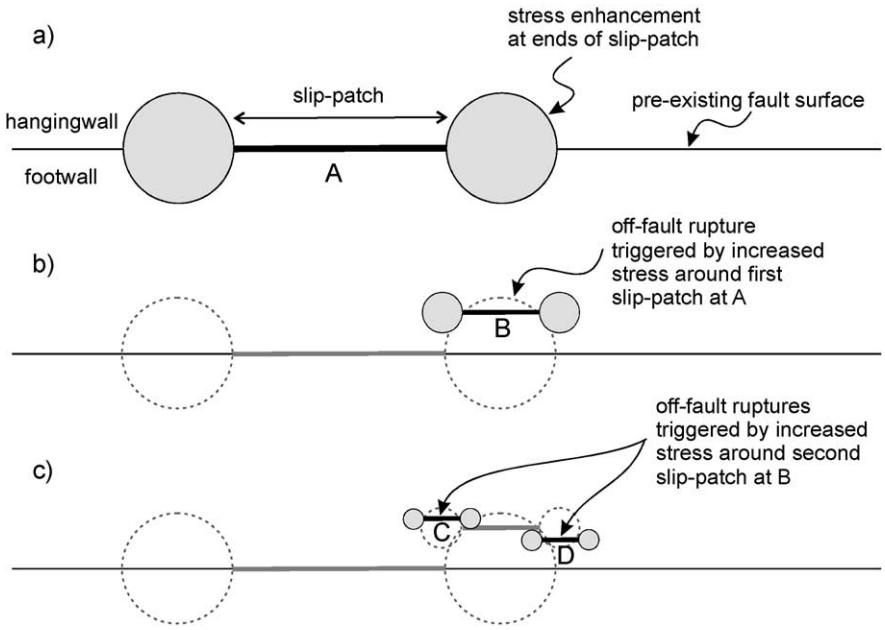

Fig. 7. Plan view cartoon of a steeply dipping normal fault showing the proposed mechanism for generating deformation at increasing distances from the fault. (a) Slip occurs on a patch of a pre-existing fault surface (the main fault plane) at point A. The grey circles indicate the zone of enhanced stress at the slip-patch tips. (b) Stress enhancement at the tips of slip-patch A induces further damage and eventual slip-patch development away from the fault at, for example, point B. (c) Stress enhancement at the tips of slip-patch B can produce further damage at C or D. If this process occurs many times as throw accumulates on the main fault plane, the resulting damage zone will be wider where the throw is greater (see text for explanation).

surfaces located nearer to the main fault plane and sparse discontinuous slip-surfaces at greater distances. It also implies a greater number of better-developed slip surfaces where fault throw is greater. All of these features of the modified slip-patch model are consistent with our field observations (Section 2). We illustrate the proposed fault growth sequence in Fig. 8 assuming, for simplicity, a constant slip-patch size on an isolated fault, which grows bilaterally. The size of the slip patch used in Fig. 8 is much smaller than the dimensions of the fault (of the order of 10%) consistent with the calculation presented above. The simple symmetrical shape of the throw profiles along the mapped faults supports the assumption that they grew primarily by bilateral propagation. Fig. 8 also illustrates variability in the extent of damage zone development that may be caused by local changes in host rock strength, related to local mineralogy and thus deformation processes.

5. Discussion

Our field observations, coupled with the slip-patch model of Cowie and Shipton (1998), suggest a new integrated model for displacement accumulation and formation of a damage zone along faults in high-porosity sandstones. We find that the evolution of the damage zone and the scaling of damage zone width with throw are strongly controlled by the deformation mechanisms operating at the grain-scale and thus the lithology and porosity of the host rock. Strain hardening is a vital component of the model proposed here, but this process is not restricted to high-porosity aeolian sandstones. Deformation bands have been found in unconsolidated sand (Heynekamp et al., 1999; Cashman and Cashman, 2000), tuffs (Wilson and Goodwin, 2001) and in accretionary prism sediments (Karig and Lundberg, 1990), and therefore the scaling of damage zone width and throw may occur in other settings.

In lithologies that do not exhibit strain hardening behaviour, the effects of the stress enhancement at slip-patch terminations could simply be superimposed, as in Fig. 6a. In this case, the deformation density would increase where the fault throw is greater (e.g. Little, 1996). Faults with extremely narrow damage zones, or even no damage zones, occur in granites (Evans et al., 2000; Lim et al., 2002; Pachell and Evans, 2002), mixed igneous rocks (Caine and Forster, 1997), mudstones (Schlische et al., 1996) and carbonates (Roberts, 1994). If the fault zone is very weak then deformation due to enhanced stress at rupture tips may preferentially take place along the fault surface rather than in the surrounding rock. For instance, the faults in granite developed along pre-existing joints that contain weak minerals (Segall and Pollard, 1983; Evans et al., 2000).

Other factors affecting damage zone width include lithological variability, fault linkage and the evolution of deformation mechanisms through time. Damage zone width can be highly variable in a heterogeneous sequence of sediments. In layered sequences, units that are more clay rich often have much narrower damage zones than sandier units (Pruatt and Reches, 1997; Heynekamp et al., 1999). Many

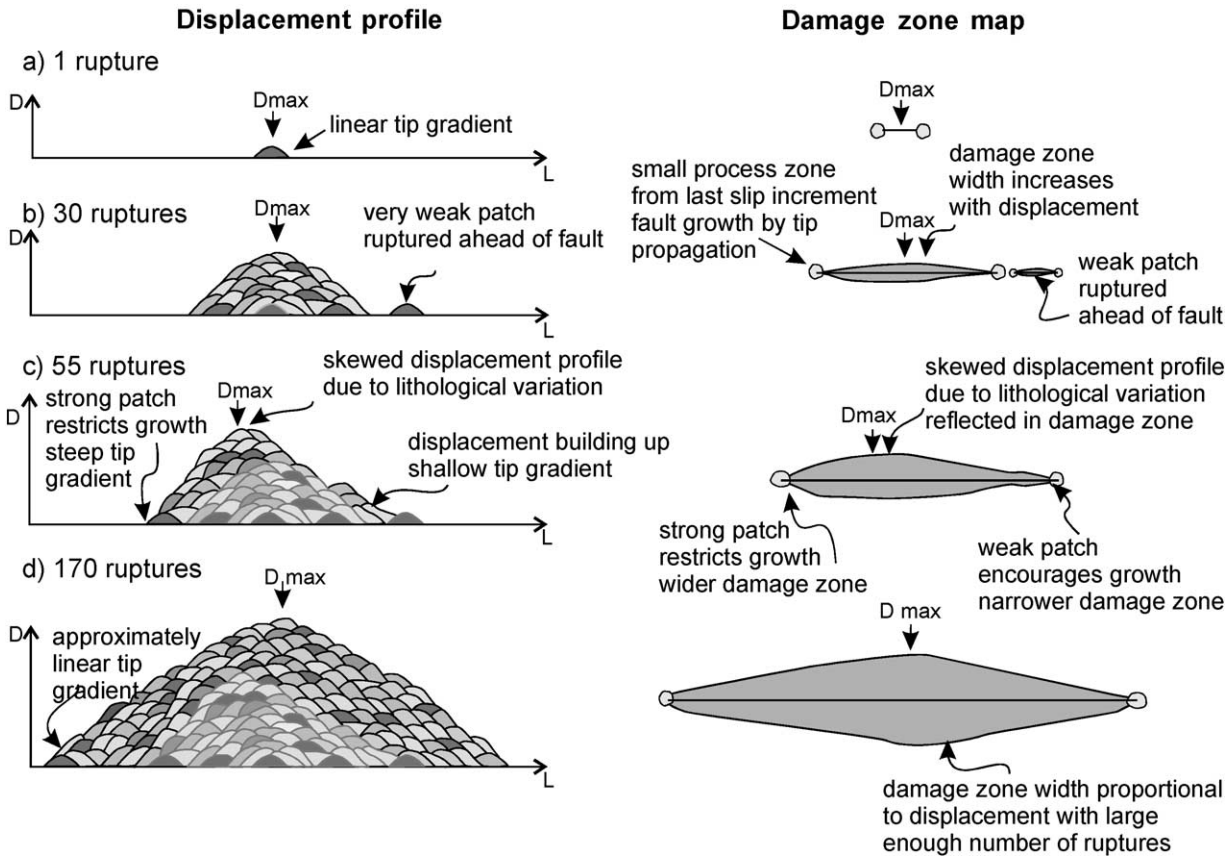

Fig. 8. Cartoon of the displacement profile and plan view of an evolving fault through time after (a) one rupture, (b) 30 ruptures, (c) 55 ruptures and (d) 170 ruptures. The displacement increment associated with each rupture is shown in a different shade of grey. For simplicity each individual rupture is drawn as if it had a symmetrical displacement profile and a circular zone of enhanced stress at its tips. This figure shows the overall widening of the damage near the centre of the fault as it propagates bilaterally and accumulates throw, following the scheme outlined in Fig. 7. Local variations in host-rock strength may cause fluctuations in damage zone width locally (see text for further details).

faults grow by the linkage of fault segments (Peacock and Sanderson, 1991; Roberts, 1996a). The modified slip-patch model that we presented here does not address this growth mechanism, but linkage is usually accommodated by the generation of cross faults and relay structures (Peacock and Sanderson, 1991). Thus increased deformation density could be expected at linkage zones or areas of complex fault geometry. The reason that damage associated with fault linkage has not been considered here is that the Big Hole and Blueberry faults show none of the characteristics of faults that have grown by linkage, e.g. displacement anomalies and changes in fault strike (Peacock and Sanderson, 1991; Dawers and Anders, 1995). Finally, deformation mechanisms may change through time, due to effects of fluid migration and mineralisation for example, producing a corresponding variation in damage zone development as a fault grows (e.g. Knipe and Lloyd, 1994).

6. Conclusions

We review detailed field observations, previously published by Shipton and Cowie (2001), of damage zone structures developed along kilometre-scale faults in the high-porosity Navajo Sandstone of central Utah. These data show a positive correlation between damage zone width and fault throw, for values of throw ranging from 0 to 30 m. This correlation, plus the orthorhombic geometry of structures in the damage zone, indicate that the damage zone has increased in width in response to displacement accumulation on the main fault surface. The damage zone consists of clusters of deformation bands and discontinuous slip-surfaces that locally accommodate minor amounts of throw (30–200 cm). In this paper we show, by applying an image analysis technique to outcrop maps, that the maximum deformation density within the damage zone has a constant value, i.e. is independent of throw.

We present a modified version of the slip-patch model for fault growth, described by Cowie and Shipton (1998), to explain the various scaling properties of the damage zones observed in our field area. We summarise the field evidence supporting the main model assumption that these faults accumulated displacement by repeated slip in patches, and demonstrate that these patches may have been a few hundred metres in size. According to our model, off-fault deformation will potentially occur in regions of high stress around the tips of each slip-patch if the stress exceeds the

yield strength of the rock. By taking into consideration the contrasting deformation mechanisms associated with forming deformation bands (local strain hardening) and slip surfaces (local strain softening) within the damage zone, we are able to explain both the widening of the damage zone with increased throw and the constant maximum deformation density. Increased deformation density occurs initially due to local strain hardening. When the deformation density within the damage zone reaches a critical value an interconnected slip-surface develops within the damage zone that begins to accumulate throw and in so doing produces more damage further away from the main fault. A hierarchy of slip-surface development is produced with greater numbers of better-developed slip-surfaces forming where the throw is larger.

In theory our approach provides a framework for understanding damage zone development around any faults and as such may be useful in prediction of sub-seismic fault architecture. However, this study demonstrates the importance of taking into consideration the host rock lithology, its porosity and the deformation mechanisms operating when interpreting or modelling fault damage zone data. This study has concentrated on characterising the damage zone geometry and displacement around relatively small-scale faults. The model presented may not apply to larger faults with a more complex history, or faults that have undergone reactivation. A more extensive study of faults across a range of different sizes, at different stages of evolution and in different host rock types is required to fully understand these effects.

Acknowledgements

This work benefited greatly from discussions with Bryne Ngwenya, Gerald Roberts and Jim Evans. Noelle Odling and Alistair Welbon provided reviews of the manuscript. Thanks to Jon Perry for help with Erdas Imagine. Jan Vermilye, John Mayers, Steve Schulz, Amy Hochberg, Kathryn Hardacre, Richard Jackson, Bertrand Maillot, Clare Bond, Kim Robeson, Jonathan Lim and Steve Thurber assisted with collecting the field data. Z. Shipton was supported by NERC studentship grant GT4/95/91/E. P. Cowie is supported by a University Research Fellowship from the Royal Society of London.

References

Antonellini, M.A., Aydin, A., 1994. Effect of faulting on fluid flow in porous sandstones: petrophysical properties. American Association of Petroleum Geologists Bulletin 78, 355–377.

Aydin, A., 1978. Small faults formed as deformation bands in sandstone. Pure and Applied Geophysics 116, 913–929.

Aydin, A., Johnson, A.M., 1978. Development of faults as zones of deformation bands and as slip surfaces in sandstones. Pure and Applied Geophysics 116, 931–942.

Aydin, A., Johnson, A.M., 1983. Analysis of faulting in porous sandstones. Journal of Structural Geology 5, 19–31.

Beach, A., Brown, J.L., Welbon, A.I., McCallum, J.E., Brockbank, P., Knott, S., 1997. Characteristics of fault zones in sandstones from NW England: application to fault transmissibility. In: Meadows, N.S., Trueblood, S.P., Hardman, M., Cowan, G. (Eds.), Petroleum Geology of the Irish Sea and Adjacent Areas. Geological Society Special Publication 124, pp. 315–324.

Beach, A., Welbon, A.I., Brockbank, P., McCallum, J.E., 1999. Reservoir damage around faults: outcrop examples from the Suez rift. Petroleum Geoscience 5, 109–116.

Bürgmann, R., Pollard, D.D., Martel, S.J., 1994. Slip distributions on faults: effects of stress gradients, inelastic deformation, heterogeneous host-rock stiffness and fault interaction. Journal of Structural Geology 16, 1675–1690.

Caine, J.S., Forster, C.B., 1997. Architecture and permeability structure of the Stillwater normal fault, Dixie Valley, Nevada. Geological Society of America Abstracts with Programs 29, 226.

Caine, J.S., Evans, J.P., Forster, C.B., 1996. Fault zone architecture and permeability structure. Geology 24, 1025–1028.

Cartwright, J.A., Mansfield, C.S., 1998. Lateral displacement variation and lateral tip geometry of normal faults in the Canyonlands National Park, Utah. Journal of Structural Geology, 20, 3–19.

Cashman, S., Cashman, K., 2000. Cataclasis and deformation band formation in unconsolidated marine terrace sand, Humboldt County, California. Geology 28, 111–114.

Chester, F.M., Logan, J.M., 1986. Composite planar fabric of gouge from the Punchbowl Fault, California. Journal of Structural Geology 9, 621–634.

Childs, C., Watterson, J., Walsh, J.J., 1995. Fault overlap zones within developing normal fault systems. Journal of the Geological Society of London 152, 535–549.

Cowie, P.A., Scholz, C.H., 1992. Physical explanation for the displacement–length relationship of faults using a post-yield fracture mechanics model. Journal of Structural Geology 14, 1133–1148.

Cowie, P.A., Shipton, Z.K., 1998. Fault tip displacement gradients and process zone dimensions. Journal of Structural Geology 20, 983–997.

Cox, S.J.D., Scholz, C.H., 1988. On the formation and growth of faults, an experimental study. Journal of Structural Geology 10, 413–430.

Crone, A.J., Haller, K.M., 1991. Segmentation and the coseismic behaviour of Basin and Range normal faults; examples from east-central Idaho and south-western Montana, USA. Journal of Structural Geology 13, 151–164.

Dawers, N.H., Anders, M.A., 1995. Displacement–length scaling and fault linkage. Journal of Structural Geology 17, 607–614.

Dawers, N.H., Anders, M.A., Scholz, C.H., 1993. Growth of normal faults: displacement–length scaling. Geology 21, 1107–1110.

Dunn, D.E., La Fountain, L.J., Jackson, R.E., 1973. Porosity dependence and mechanisms of brittle fracture in sandstones. Journal of Geophysical Research 78, 2403–2417.

Evans, J.P., Shipton, Z.K., Pachell, M.A., Lim, S.J., Robeson, K., 2000. The structure and composition of exhumed faults, and their implications for seismic processes. In: Bokelmann, G., Kovach, R.L. (Eds.), Proceedings of the 3rd Conference on Tectonic Problems of the San Andreas Fault System. Stanford University Publications, Geological Sciences 21, pp. 67–81.

Fossen, H., Hesthammer, J., 2000. Possible absence of small faults in the Gullfaks Field, northern North Sea: implications for downscaling of faults in some porous sandstones. Journal of Structural Geology 22, 851–863.

Gupta, A., Scholz, C.H., 2000. A model of normal fault interaction based on observations and theory. Journal of Structural Geology 22, 865–879.

Heynekamp, M.R., Goodwin, L.B., Mozley, P.S., Haneberg, W.C., 1999. Controls on fault zone architecture in poorly lithified sediments, Rio Grande Rift, New Mexico: implications for fault zone permeability and fluid flow. In: Haneberg, W.C., Mozley, P.S., Moore, C.J., Goodwin, L.B. (Eds.), Faults and Subsurface Fluid Flow, American Geophysical Union Geophysical Monograph 113, pp. 27∇d49.

Hodgkinson, K.M., Stein, R.S., King, G.C.P., 1996. The 1954 Rainbow

Mountain–Fairview Peak–Dixie Valley earthquakes: a triggered normal faulting sequence. Journal of Geophysical Research 101, 25459–25471.

Jamison, W.R., Stearns, D.W., 1982. Tectonic deformation of Wingate sandstone, Colorado National Monument. American Association of Petroleum Geologists Bulletin 66, 2584–2608.

Karig, D.E., Lundberg, N., 1990. Deformation bands from the toe of the Nankai accretionary prism. Journal of Geophysical Research 95, 9099–9109.

King, G.C.P., Stein, R.S., Lin, J., 1994. Static stress changes and the triggering of earthquakes. Bulletin of the Seismological Society of America 84, 935–953.

Knipe, R.J., Lloyd, G.E., 1994. Microstructural analysis of faulting in quartzite, Assynt, NW Scotland: implications for fault zone evolution. Pure and Applied Geophysics 143, 229–254.

Knipe, R.J., and nine others, 1998. Fault seal analysis: successful methodologies, applications, and future directions. In: Moeller-Pederson, P., Koestler, A.G. (Eds.), Hydrocarbon Seals, Importance for Exploration and Production, Norsk Petroleum Society Special Publication 7, pp. 15–38.

Knott, S.D., Beach, A., Brockbank, P.J., Brown, J.L., McCallum, J.E., Welbon, A.I., 1996. Spatial and mechanical controls on normal fault populations. Journal of Structural Geology 18, 359–372.

Krantz, R.W., 1988. Multiple fault sets and three-dimensional strain: theory and application. Journal of Structural Geology 10, 225–237.

Lim, S.J., Evans, J.P., Hestir, K., Yang, J., 2002. Three-dimensional structure of small strike-slip faults: inferences from field data and stochastic modelling. Journal of Structural Geology in press.

Little, T.A., 1996. Faulting-related displacement gradients and strain adjacent to the Awatere strike-slip fault in New Zealand. Journal of Structural Geology 18, 321–342.

McGrath, A.G., Davison, I., 1995. Damage zone geometry around fault tips. Journal of Structural Geology 17, 1011–1024.

Machette, M.N., Personius, S.F., Nelson, A.R., Schwartz, D.P., Lund, W.R., 1991. The Wasatch fault zone, Utah—segmentation and history of Holocene earthquakes. Journal of Structural Geology 13, 137–149.

Main, I., Mair, K., Kwon, O., Elphick, S., Ngwenya, B., 2001. Experimental constraints on the mechanical and hydraulic properties of deformation bands in porous sandstones: a review. In: Holdsworth, R.E., Strachan, R.A., Magloughlin, J.F., Knipe, R.J. (Eds.), The Nature and Significance of Fault Zone Weakening, Geological Society of London Special Publication 186, pp.43–63.

Mair, K., Main, I., Elphick, S., 2000. Sequential growth of deformation bands in the laboratory. Journal of Structural Geology 22, 25–42.

Martel, S.J., Boger, W.A., 1998. Geometry and mechanics of secondary fracturing around small three-dimensional faults in granitic rock. Journal of Geophysical Research 103, 21299–21314.

Martel, S.J., Pollard, D.D., 1989. Mechanics of slip and fracture along small strike-slip fault zones in granitic rock. Journal of Geophysical Research 94, 9417–9428.

Muraoka, H., Komata, H., 1983. Displacement distribution along minor fault traces. Journal of Structural Geology 5, 483–495

Myers, R.D., Aydin, A., 1998. Fault damage distribution, evolution, and scaling in porous sandstones. Geological Society of America Abstracts with Programs 30 (7), 63.

Nicol, A., Walsh, J.J., Watterson, J., Childs, C., 1996. The shapes major axis orientations and displacement patterns of fault surfaces. Journal of Structural Geology 18, 235–248.

Pachell, M.A., Evans, J.P., 2002. Growth, kinematics, and internal structure of an exhumed 10-kilometer-long left-lateral strike-slip fault in granitic rocks, central Sierra Nevada, California. Journal of Structural Geology in press.

Peacock, D.C.P., Sanderson, D.J., 1991. Displacement, segment linkage and relay ramps in normal fault zones. Journal of Structural Geology 13, 721–733.

Pollard, D.D., Segall, P., 1987. Theoretical displacements and stresses near fractures in rock: with applications to faults joints, veins, dikes and solution surfaces. In: Atkinson, B. (Ed.). Fracture Mechanics of Rock. Academic Press, London, pp. 277–349.

dePolo, C.M., Clark, D.G., Slemmons, D.B., Ramelli, A.R., 1991. Historical surface faulting in the Basin and Range province, western North America: implications for fault segmentation. Journal of Structural Geology 13, 123–136.

Pruatt, M.A., Reches, Z., 1997. 3D structure at strike-slip fault ends in a layered clastic sedimentary sequence, San Rafael Swell, Utah. Geological Society of America Abstracts with Programs 29 (6), 199.

Reches, Z., 1983. Faulting of rocks in three-dimensional strain fields II, theoretical analysis. Tectonophysics 95, 133–156.

Roberts, G.P., 1994. Displacement localisation and palaeo-seismicity of the Rencurel Thrust Zone, French Sub-Alpine Chains. Journal of Structural Geology 16, 633–646.

Roberts, G.P., 1996a. Variation in fault slip directions along active and segmented normal fault systems. Journal of Structural Geology 18, 835–845.

Roberts, G.P., 1996b. Noncharacteristic normal faulting surface ruptures from the Gulf of Corinth, Greece. Journal of Geophysical Research 101, 25255–25267.

Schlische, R.W., Young, S.S., Ackerman, R.V., Gupta, A., 1996. Geometry and scaling relations of a population of very small rift related normal faults. Geology 24, 683–686.

Scholz, C.H., 1990. Mechanics of Earthquakes and Faulting. Cambridge University Press.

Scholz, C.H., Dawers, N.H., Yu, J.Z., Anders, M.H., 1993. Fault growth and fault scaling laws: preliminary results. Journal of Geophysical Research 98, 21951–21961.

Segall, P., Pollard, D.D., 1983. Nucleation and growth of strike-slip faults in granite. Journal of Geophysical Research 88, 555–568.

Shipton, Z.K., 1999. Fault displacement profiles and off-fault deformation: interpreting the records of fault growth at the Chimney Rock fault array, Utah, USA. PhD thesis, Edinburgh University.

Shipton, Z.K., Cowie, P.A., 2001. Analysis of three-dimensional damage zone development over a micron to km scale range in the high-porosity Navajo sandstone, Utah. Journal of Structural Geology 23, 1825–1844.

Shipton, Z.K., Evans, J.P., Robeson, K., Forster, C.B., Snelgrove, S., 2002. Structural heterogeneity and permeability in faulted aeolian sandstone: implications for subsurface modelling of faults. American Association of Petroleum Geologists Bulletin 86, 863–883.

Stein, R.S., Lisowski, M., 1983. The 1979 Homestead Valley earthquake sequence, California; control of aftershocks and postseismic deformation. Journal of Geophysical Research 88, 6477–6490.

Vermilye, J.M., Scholz, C.H., 1998. The process zone: a microstructural view. Journal of Geophysical Research 103, 12223–12237.

Wallace, R.E., Morris, H.T., 1986. Characteristics of faults and shear zones in deep mines. Pure and Applied Geophysics 124, 105–125.

Wilson, J.E., Goodwin, L.B., 2001. Deformation bands and fluid-fault interaction in non-welded tuffs. Earth Systems Processes, Edinburgh, Scotland, Programmes with Abstracts, p. 50.